3D-printed sound absorbers: compact and customisable at broadband frequencies

Setaki, F.; Tian, F.; Turrin, M.; Tenpierik, M.J.; Nijs, L.; van Timmeren, A.

DOI
10.1007/s44150-023-00086-9

Publication date
2023

Document Version
Final published version

Published in
Architecture, Structures and Construction

Citation (APA)
Setaki, F., Tian, F., Turrin, M., Tenpierik, M. J., Nijs, L., & van Timmeren, A. (2023). 3D-printed sound absorbers: compact and customisable at broadband frequencies. *Architecture, Structures and Construction*, *3*(2), 205-215. https://doi.org/10.1007/s44150-023-00086-9

Architecture, Structures and Construction (2023) 3:205–215
https://doi.org/10.1007/s44150-023-00086-9

ORIGINAL PAPER

3D-printed sound absorbers: compact and customisable at broadband frequencies

F. Setaki[1] · F. Tian[2] · Michela Turrin[1] · M. Tenpierik[1] · L. Nijs[1] · A. van Timmeren[1]

Received: 1 August 2022 / Accepted: 1 February 2023 / Published online: 16 February 2023

Abstract
This paper discusses a novel, compact sound absorption solution with high performance at various frequencies, including low frequencies, achieved through the effective use of Computational Design and Additive Manufacturing (AM). Sound absorption is widely applied for reducing noise and improving room acoustics; however, it is often constrained by conventional design, material properties and production techniques, which offer limited options for customising performance. This research highlights that AM, in combination with computational design tools, can support the development of novel sound-absorbing products with high performance based on the principle of viscothermal wave propagation in prismatic tubes. The potential of these designs was explored via two studies of customised sound-absorbing panels whose performance was measured in a reverberation room. A custom measurement technique was used based on logarithmic sweeps with high-resolution FFT analysis. A comparison of the measurement results with the theory of viscothermal wave propagation indicated good agreement; thus, this study demonstrates the possibility of developing new concepts and design methods for novel room acoustic devices.

Keywords 3D printing · Additive manufacturing · Customisation · Sound absorption · Broadband

Introduction

Sound absorption technologies are broadly used to reduce noise and improve room acoustics. Despite their wide range of applications, these technologies are often constrained by conventional design and production techniques and thus cannot meet the growing need for customisation, optimised performance and complex shapes. In addition, typical solutions are difficult to use for low-frequency damping due to their large size or volume, their extreme narrowband performance or their vulnerability to dust and water [3, 6].

These limitations can be potentially addressed by applying Additive Manufacturing (AM) technologies to the production of sound absorbers. The term AM describes a family of fabrication technologies that can produce parts in a layered manner, broadly known as 3D printing. The advantages of these technologies include their ability to produce parts with high geometric complexity at high resolution (up to mm size) without the use of moulds. Bypassing the constraints of traditional manufacturing approaches by introducing AM processes to acoustic device production supports the development of mono-material structures with improved sound absorption and customisability. In addition, using AM technology can facilitate the development of sustainable solutions for robust sound absorbers that are tuned for broad frequency ranges. Because they are highly customisable, these structures can be easily integrated into building components, machines or furniture. Furthermore, the design freedom of AM technologies can be used to create engineered structures that are designed based on sound-absorbing mechanisms and thus perform better than conventional absorbers. Many acoustic materials are vulnerable to dust and are not washable because of their porous nature. However, acoustic panels produced with 3D printing can be more readily engineered to be water resistant thanks to the solid surface of their geometry; hence, they can be more easily cleaned. This can be useful in settings where dirt is an issue, such as areas for children or hospitals. AM also facilitates the possibility of creating compact solutions for applications where space efficiency is important, e.g. in working cabins or aircraft.

✉ F. Setaki
f.setaki@tudelft.nl

[1] Faculty of Architecture and the Built Environment, Delft University of Technology, Delft, The Netherlands

[2] School of Aerospace Engineering, Huazhong University of Science and Technology, Wuhan, China

However, in addition to the benefits of AM, there are also challenges. The texture of the final surface has a layered character that is visible to the naked eye and may affect the acoustic properties of the surface. Furthermore, the microporosity of most printed materials is hard to control and cannot be entirely avoided; therefore, it is sometimes difficult to achieve a constant quality of printed parts. AM materials are also often not UV-resistant, and their costs are still relatively high. Additionally, although micro- and macro-scale sound-absorbing structures are well-suited to the manufacturing capabilities of most AM processes, the complexity of the features may cause problems in removing support material, especially when the cavities or pores become practically inaccessible. For certain geometries, the post-processing step might become difficult or time-consuming.

The potentials of the combination of AM with sound absorbing mechanisms are relatively unexplored; to date, applications remain limited to small-scale prototypes, measured only in impedance tubes [5, 7]. Further, no research to date has tested the performance of larger AM sound-absorbing panels in a reverberation room. Existing examples of larger prototypes mostly address other acoustic strategies such as diffusion [12, 13]. In terms of customisation in acoustics, existing studies focus primarily on alternative production techniques, such as subtractive, moulding or bending techniques [17] or 3D printing is used in scaled models [9]. However, the diffusion of AM in acoustic applications is expected to increase in the coming years, due to the fast development and increasing affordability of AM technology and its corresponding advantages, such as the customisation possibilities and material properties described above.

This study investigates the possibility of achieving compact broadband sound absorption at low frequencies by focusing on the development of quarter-wavelength resonators. The performance of such resonators relies mostly on their geometric characteristics, such as the length and the diameter of the tube; hence, their acoustic performance can be controlled by their shape, enabling the performative design of custom sound-absorbing elements. In quarter-wavelength tube resonators, the incident waves are cancelled by the waves in the resonator and damped by viscothermal loss in the resonator [4]. This resonator type is typically effective in narrowband noise problems; however, solutions that address a wide frequency range are most commonly required in room acoustics. Here, it will be shown that these resonators' effects can be improved by combining multiple resonators that are tuned for different frequencies, which can be used to achieve broadband sound absorption. This acoustic concept is: (1) optimised and designed with a computational workflow developed by the research team [15], (2) produced with AM by Materialise and (3) assessed with measurements of two different panels in a reverberation room using a newly developed measurement analysis technique. As part of this project, it was essential to develop optimisation and design computational tools to provide customised design solutions with predictable sound-absorbing performance. The computational tool developed for the needs of the project was beta-tested as part of the two case studies. In both panel studies, a given geometry was tuned for selected broadband absorption at low frequencies. In each case, a large sound-absorbing surface was produced with AM, using Selective Laser Sintering (SLS) and Polyamide (PA12) as a material. The prototypes were measured and assessed in the diffused field of the reverberation room at TU Delft using a novel method developed within this project.

Methods

Design of optimised sound-absorbing surfaces

The design process began with the preparation of the acoustic surface based on the model of Zwikker and Kosten for viscothermal wave propagation in prismatic tubes [18], which has also been validated for 3d printed material [14]. The goal of the process was to design an acoustic item customised for given frequencies (or a frequency range) that meets given dimensions (the available area of the acoustic panel). The design process was supported by computational methods and related tools, two of which were specifically developed in this research project, based on a two-step approach.

The first step involves identifying the appropriate number of tubes and their radii and lengths to maximise the absorption coefficient for a given range of frequencies in a given space. The process is structured as an optimisation problem, where the optimal combination of tubes is searched with the target of achieving an absorption coefficient as close to 1 as possible. The design variables in this optimisation are the number of tubes, their radii and their lengths. The performance (fitness) assessment can be performed using different methods depending on the desired accuracy: for fast calculations, an acoustic calculation formula is used, which requires the kelvin temperature, relative humidity, ambient pressure and other parameters as constant inputs. The process is encoded in a component integrated into the Rhino/Grasshopper (McNeel) software environment.

The second step involves generating the 3D geometry of the acoustic panel with the aim of production by 3D printing. This process is structured as an automated algorithmic generation of 3D geometric features, using the outputs of the optimisation step and a given 3D surface freely modelled by the designer as inputs. The process is encoded in a component integrated into the Rhino/Grasshopper (McNeel) software environment as a Tool for Acoustic Design Optimisation (TADO). The TADO is based on an algorithm that packs tubes with circular profiles on a given surface in an

offset layout. The offset follows the outline (curve) and surface of the panel in any shape. Accordingly, the TADO user can freely customise the form of the panels yet still design an acoustic item optimised for absorbing the desired frequencies or frequency range. The bending and packing of the tubes result in a spatially compact solution. In addition to the numeric values derived from the optimisation, the additional inputs in this step are: (1) the boundary representation base geometry of the panels, (2) the axial and parallel distances between the tubes and (3) the wall thickness of the tubes. The output geometry consists of the base panel and integrated tubes, which are packed such that they are spatially optimised and can be manufactured by AM.

The above research workflow was followed for the study of two different panels. Both panels are large 3D-printed acoustic surfaces tuned for broadband low-frequency sound absorption between 240 and 315 Hz. The main difference between the two panels is that the first 3D-printed acoustic surface is flat and the second is curved. Accordingly, two different versions of TADO were developed for the automated generation of the sound-absorbing panels: (1) TADO1 for flat surfaces and (2) TADO2 for 3D surfaces; hence, case study 1 tests TADO1 and case study 2 tests TADO2.

Fabrication of optimised sound-absorbing surfaces

The output geometry was produced with the SLS technique and PA12 (a type of polyamide). The aspect of environmental sustainability is important in the decision to use SLS. This option is more sustainable as PA12 is recyclable [16]. In addition, SLS can potentially minimise production waste by reusing the un-sintered powder [8]. However, this technology is more expensive and more difficult to apply to large prints, especially in comparison to FDM printing or conventional production techniques. An alternative approach is the use of stereo-lithography, which is easier and more cost-effective but might be less sustainable due to its use of non-recyclable resins. The porosity of SLS-printed parts ranges from 2–12%, from closed cell up to open cell porosity. The amount of porosity depends on the bulkiness of the print: the bulkier the print, the lower its porosity. Previous impedance tube measurements made by this study's research team showed that the 3D-printed material acts mostly as a reflective surface [14]. This feature is highly beneficial for resonant absorbers that rely mostly on geometrical characteristics.

After generating the geometry using the TADO, the geometry must be sliced before printing. The optimum layer orientation of the prints is chosen to reduce printing hours and maximise the printing capacity of the printing bed. The size of the printing bed (WxLxH: 650 × 330x560 m) defines the maximum size of the printed sample. SLS is a powder-based technique; using this approach to fabricate the bent tubes allows complex structures to be made without the need for support structures that are hard to remove and require extensive post-processing. In SLS, the dimensional tolerance is expected to be ± 0.3% with shrinkage in the 2–3% range [1]; thus, only minimal impact is expected on the manufactured components' acoustic performance. Limitations arising from the fabrication technique include: (1) the minimum radius size (the suggested minimum tube radius was 5 mm, given a wall thickness of 2 mm) and (2) the bending angle of the tubes. If the geometry is bent to follow sharp corners, it is difficult to remove the powder.

Measurements in the reverberation room

A major challenge in this research project was to define an appropriate method for measuring the 3D-printed acoustic surfaces. In the early phases of this research, small samples were measured in a B&K4206 impedance tube for normal sound incidence; these results will be reported in another paper. For large samples, measurements are generally performed in a reverberation room according to [10]. Measurements were performed in the reverberation room at the Faculty of Applied Sciences at the Delft University of Technology, which is compliant with ISO 354. During the measurements, the source was placed at two positions and microphones were placed at five positions, resulting in 10 spatially independent measured decay curves. A logarithmic sweep signal was used for excitation of the room (four signals per measurement point) and the results of the measured reverberation times were averaged over the 10 distinct measurements.

A Norsonic Nor140 class 1 sound analyser was used as a microphone and a Norsonic Nor276 omnidirectional sound source connected to a Norsonic Nor280 power amplifier was used as a source. Both the source and receiver were connected to a laptop via a Behringer UCA222 audio interface. On the laptop, a program written in MATLAB was running; this program was used for sending out the sweeps, recording the input signals and analysing the results.

The measurements were first performed in an empty chamber as a reference. The sound absorber was then placed in the middle of the room on the floor and measured with open and closed exposed ends. The sealing of the tubes (on the exposed side) was achieved by placing clay at their orifices. By cross-comparing the measurements of the room made in the three settings (i.e. empty, open and closed tubes), detailed conclusions can be made regarding the panels' acoustic performance.

The acoustic field in the reverberation room in this study is diffused and enables absorption coefficients to be obtained with high precision. However, according to ISO 354 m the impulse response should be analysed with FFT (Fast Fourier Transform) analysis and filtered for 1/3rd octave bands. The disadvantage of this analysis approach is that frequency details

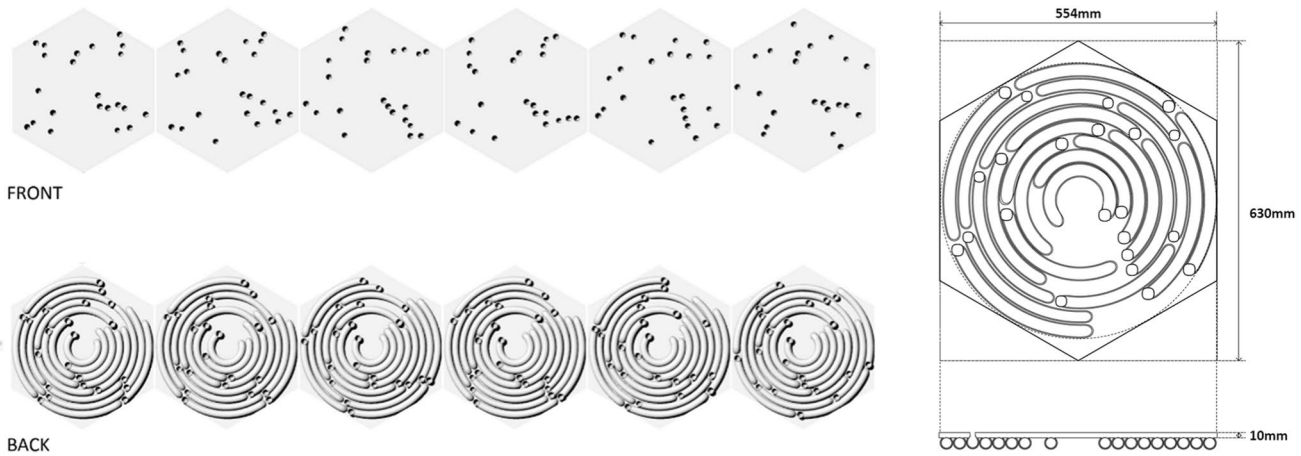

Fig. 1 [LEFT]Front and back view of case study 1 panels. [RIGHT] dimensions of case study 1 panels

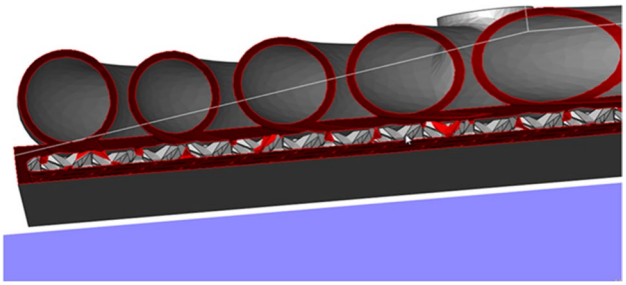

Fig. 2 Hollowed parts with a 3 mm wall thickness and infill structure to avoid overheating/deformation

may be lost in the 1/3rd octave band filtering as narrowband absorption peaks are sometimes missed. To overcome this, the results were filtered for both 1/3rd and 1/27th octave bands. The 1/27th octave band results must be interpreted with caution because of potential decay artefacts and the room's inadequate spectral density for low frequencies. The diffuse field sound absorption coefficient was calculated based on the measured T-20 (20 dB decay from -5 dB to -25 dB below the peak level).

An additional deviation from standard practice regarding measurements in the reverberation room includes the size of the acoustic panel surface tested. Typically, measurements in a reverberation room of 200 m^3 require a sample size of 10–12 m^2. Due to resource limitations (high costs for producing the samples with SLS), the sample size in this study was limited to slightly above 2 m^2. This is smaller than the required area according to ISO 354 and may have an impact on the accuracy of the results. [2] explored the impact of sample area on the sound absorption coefficient of an 8 cm-thick porous absorber measured in a reverberation room by varying the sample size from 1 to 12 m^2; their findings indicate that the sound absorption coefficient for many octave bands became relatively stable at sample areas of 4 to 5 m^2 and above. The focus frequencies of our research are 200–315 Hz. For the 250 Hz octave band, Carvalho [2] found a difference of approximately 0.1 for the absorption coefficients between 2 m^2 and 12 m^2 samples. According to [11], the sample size is not expected to have a significant impact on the results. Therefore, it is expected that the small sample size in this study will impact the value of the absorption coefficient to some extent but will have minimal impact on the frequency of the absorption peaks.

Case studies

Case study 1 – broadband absorber at low frequencies: flat panel

Design and fabrication of optimised sound-absorbing surface

This case study involves optimising a flat sound-absorbing surface for low frequencies. The inputs for the acoustic optimisation process were the total surface area of the panels (2.06 m^2) and the selected target frequency range (240–315 Hz). The results of the acoustic calculation produced a set of 192 tubes with a total sum length of 58.1 m and an average radius of 10.86 mm. The optimised output geometric features are shown in Table 1 (left).

Before inputting this data into the TADO1, the geometry of the acoustic surface must be defined. Given the total area of the acoustic surface and the dimensions of the boundary box of the SLS printer, the acoustic surface was tessellated into eight equally sized, hexagonal, flat panels with external dimensions of 630 × 545 mm and 10 mm thickness.

In the next step, the geometry of the panels and the numeric data for the acoustic calculation are inserted into TADO1 to automatically generate 3D models of the eight acoustic panels and optimally pack the 58.1 m-long

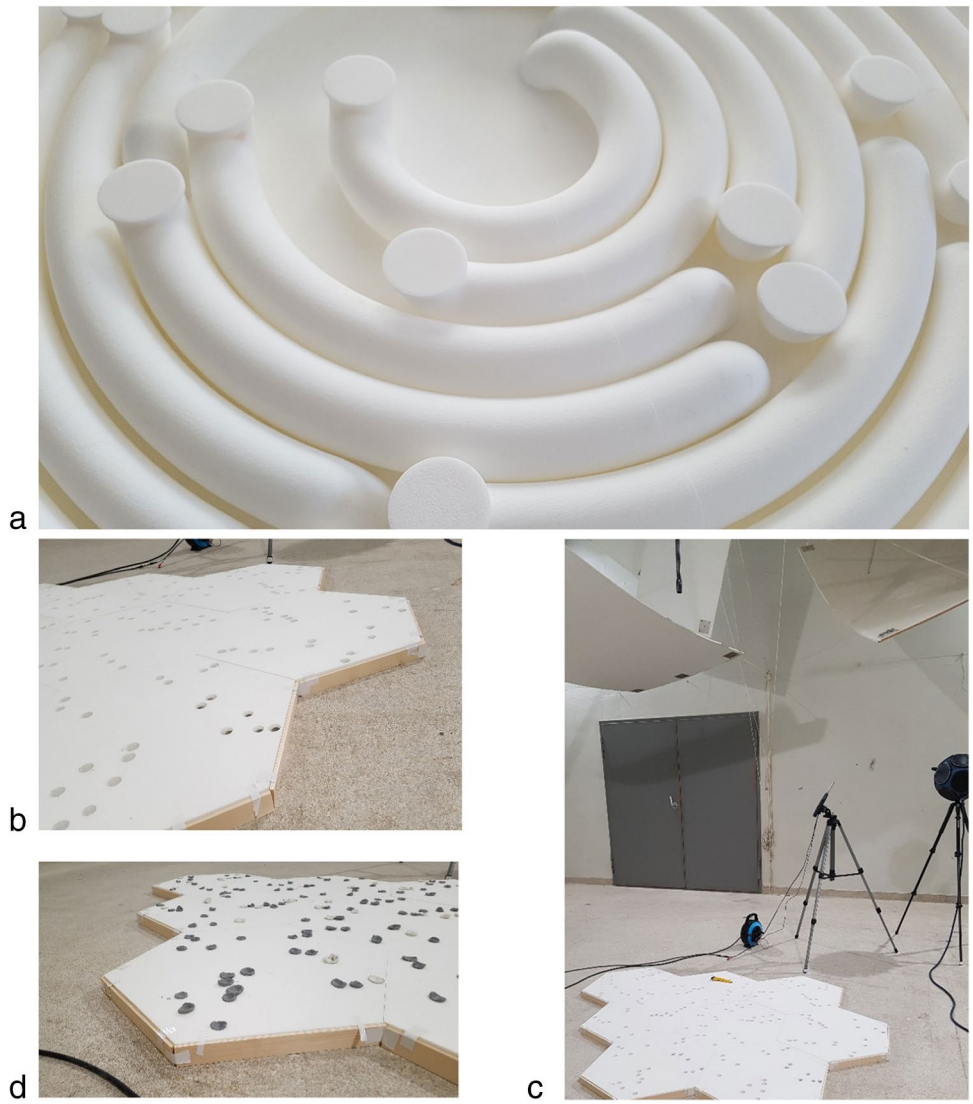

Fig. 3 Case Study 1 [**A**] Printed prototype, [**B**] Layout: open tubes, [**C**] Prototypes are installed in the reverberation room and [**D**] Layout: closed tubes, where the orifices of the tubes are sealed with clay

Table 1 [LEFT] results from acoustic optimisation in Rhino/ Grasshopper define the number, radius and length of tubes per frequency. [RIGHT] number of tubes per frequency per panel type (A, B or C)

Input		Output			Distribution of tubes/ panel		
Total surface [m^2]	frequency [Hz]	radius [mm]	length [mm]	number of tubes	Panel A	Panel B	Panel C
2.06	240	11.44	347.01	34	5	4	0
	255	10.08	326.75	37	6	1	0
	270	11.05	304.52	25	4	1	0
	285	11.61	291.05	36	6	0	0
	300	10.61	275.82	28	1	18	4
	315	10.37	262.54	32	0	2	30

prismatic tubes. Additionally, the axial and parallel distances (both 1 mm) and the wall thickness (2 mm) are inserted. This process results in three different panel typologies (A, B and C). Although panel A needs to be produced six times, each of the 'copies' is unique in terms of its geometry due to the differentiated sequence and position of the packed tubes. Panels B and C are each printed once. Table 1 (right) shows the distribution of the resonators per panel.

The finalised geometry was prepared for 3D printing (Fig. 1). To reduce overheating and deformation, the geometry of the panels was hollowed with a 3 mm wall thickness. Additionally, an infill structure was integrated, as shown

in Fig. 2. The parts were oriented vertically in the printing bed and nested in groups of four panels per printing bed.

The powder-based nature of SLS is beneficial for this project because there is no need for additional support structures that would increase the post-production time. The long, narrow and complex nature of the tubes causes difficulties in removing un-sintered powder and verifying that the samples are completely cleared. For this reason, the closed end of the back side is designed to be removable to assist in post-processing using compressed air. Tolerances in the production of the samples are difficult to measure due to the complexity of the printed geometry.

Measurements in the reverberation room

The panels were placed on the floor in the middle of the reverberation room. To minimise the effects of the edges and the partially open air cavity underneath the panels, the sides of the absorbing panels were sealed on the ground with wooden slats along their perimeter (Fig. 3).

From the obtained measurements, the sound absorption coefficient of the 3D printed surface in a diffuse field can be derived. To better understand the measured performance, coefficient curves were calculated for three different conditions: (1) open tube measurements relative to closed tube measurements, (2) closed tube measurements relative to the empty room and (3) open tube measurements relative to the empty room. Condition (3) is normally used in the ISO 354 standard. Figure 4 shows the sound absorption coefficient as calculated based on the measured decay curve for T-20. The results for the open tubes relative to an empty room (green curve in Fig. 4) show broadband absorption at the targeted frequency range (240–315 Hz) that matches with theory, even though individual peaks as calculated cannot

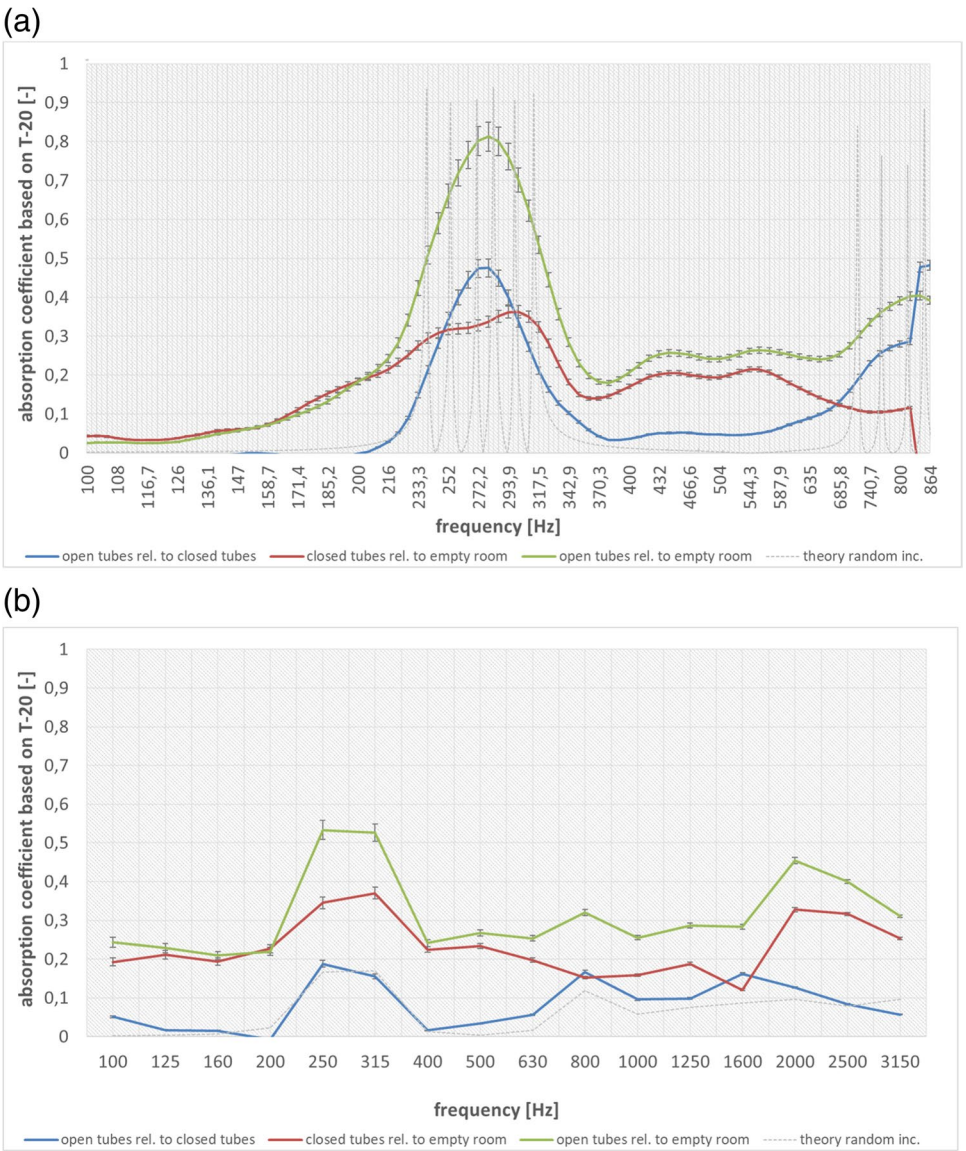

Fig. 4 Case Study 1: measured vs calculated performance of the sound absorption coefficient analysed in (**a**) 1/27th octave bands and (**b**) 1/3rd octave bands. The theoretical curves in the 1/27th octave bands graph are based on a continuous theoretical function and in the 1/3rd octave band graphs are filtered for 1/3rd octave bands

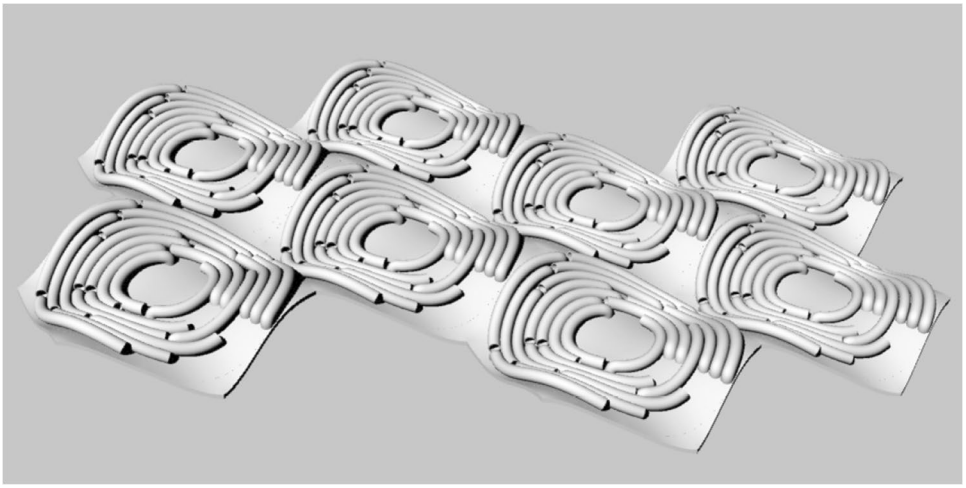

Fig. 5 3D view of Case Study 2 panels

be discerned. This is to be expected given the diffused field in the room and the generally slightly higher damping inside such systems than calculated.

Furthermore, the observed sound absorption coefficient values are around 0.1/0.2 and 0.2/0.3 respectively at frequencies below and above the targeted band. This implies that the non-prismatic parts of the acoustic surface (i.e. the flat surface) also display sound-absorbing behaviour. The red curve in Fig. 4 (closed tubes relative to the empty room) shows the exact amount of panel absorption by eliminating the effect of the tubes by sealing their entrances with clay. A wide peak is noticeable at frequencies of 185–290 Hz, which can likely be attributed to the panel resonance of the flat surface.

By comparing the results of the open and the closed tubes (Fig. 4– blue line), the flat surface absorption effect can be eliminated, thus isolating the sound absorption coefficient of the specific tube layout. The results in Fig. 4 indicate that the measured peak frequencies coincide with the expected results from the theory; however, the peaks are wider and lower. This phenomenon may be potentially explained by deviations in the printed geometry, measurement inaccuracy and 1/27th octave band filtering or the relatively small size of the sample compared to the volume of the room (200 m^3). In addition, above approximately 690 Hz, increased sound absorption can be observed, which is also consistent with the theory.

Case study 2 – broadband absorber at low frequencies – Exploiting the 3D possibilities of AM

Design and fabrication of an optimised sound-absorbing surface

In the second case, the 3D potential of the AM technique was explored in combination with the developed workflow. To make the two cases comparable, the first part of the acoustic optimisation calculated via the TADO remains the same. Thus, the numeric input (surface area of 2.06 m^2 and target frequency range of 240–315 Hz) and, consequently, the output (192 tubes with a total sum length of 58.1 m and average radius of 10.86 mm) remain the same.

The geometry generation step was automated using TADO2. The input geometry of the panel is based on the same hexagonal outline of panels from case 1; however, their sides are sculpted to create a double-curved surface. Due to the 3D nature of the base geometry, the radial (13 mm) and axial (9 mm) distances between the tubes needed to be increased to avoid self-intersecting geometries. The geometry of the 3D panel can be enclosed in a box with dimensions 630 × 545x145 mm^3. In case 1, the panel resonance was observed in a frequency range from 180–290 Hz. To reduce this effect, the mass of the acoustic surface in case 2 was increased by increasing the thickness of the curved surface of the panels to 20 mm and the thickness of the tubes to 3 mm. This process resulted in 10 unique panel geometries, each containing an average of 19 tubes (Fig. 5).

Before printing, the final geometry was hollowed using a standard outer wall thickness of 3 mm. To reduce further deformation, an internal honeycomb structure was inserted with a cell size of 15 mm and an inner wall thickness of 1.5 mm. This inclusion positively affects the dimension accuracy and powder removal of the tubes. Furthermore, mechanical connections between the different panels were integrated into the geometry, consisting of two parts: (1) a sliding notch (Fig. 6 right) and (2) holes for the tie-ups. The dimensions of the notch derive from the panel geometry and its proportions; hence, the width was defined as 1/3rd of the plate thickness, with depths varying from 5 to 10 mm depending on the geometry of the plate. The male and female notches were designed with a clearance of 0.3 mm for glueing.

The parts were oriented vertically in the printing bed and were nested in groups of two panels per printing bed (Fig. 7).

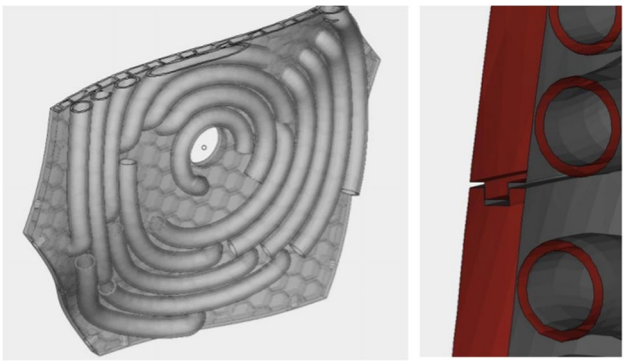

Fig. 6 [LEFT] Inner honeycomb structure for reducing warping during printing; [RIGHT] Connection detail of the sliding notch with 0.3 mm clearance

The larger volume of the panels increased the production cost. The un-sintered powder was not removed (it remains in the component), except from inside the tubes (Fig. 6 Left).

The global dimensions of the printed panels deviated from the drawings. Specifically, the measured tolerance ranges were 0.3–1.3% per side, with an average tolerance of 0.51% (Figs. 8). This relatively small inaccuracy in the dimensions affects the assembly of the surface by leaving small gaps along the joints.

Measurements in the reverberation room

The panels were placed in the middle of the reverberation room (Fig. 9). The seams between the panels were sealed with clay. Due to the complex shape of the panels, the sides on the perimeter of the panels remained unsealed, as this layout better represents the installation mode in space. However, because these open edges will impact reverberation, in the analysis, we mostly compare the panels with open tubes to those with the tubes closed off. From the measurements, the sound absorption coefficient of the 3D printed surface in

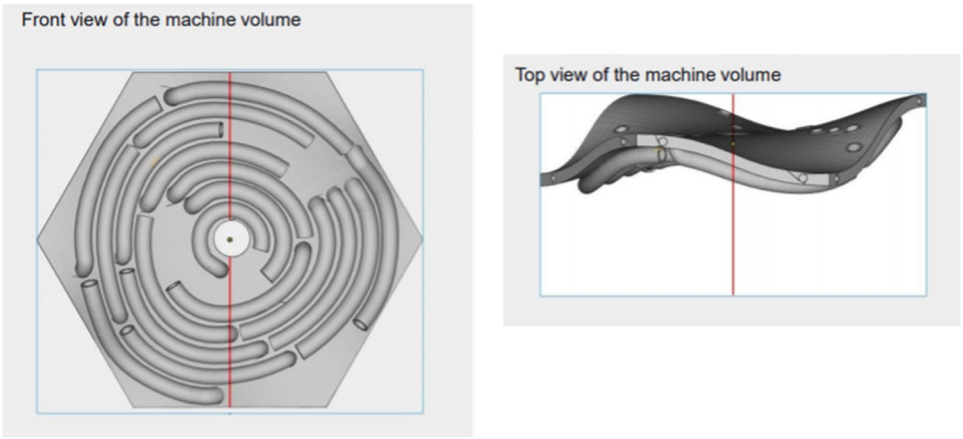

Fig. 7 Orientation of the panel in the printing bed

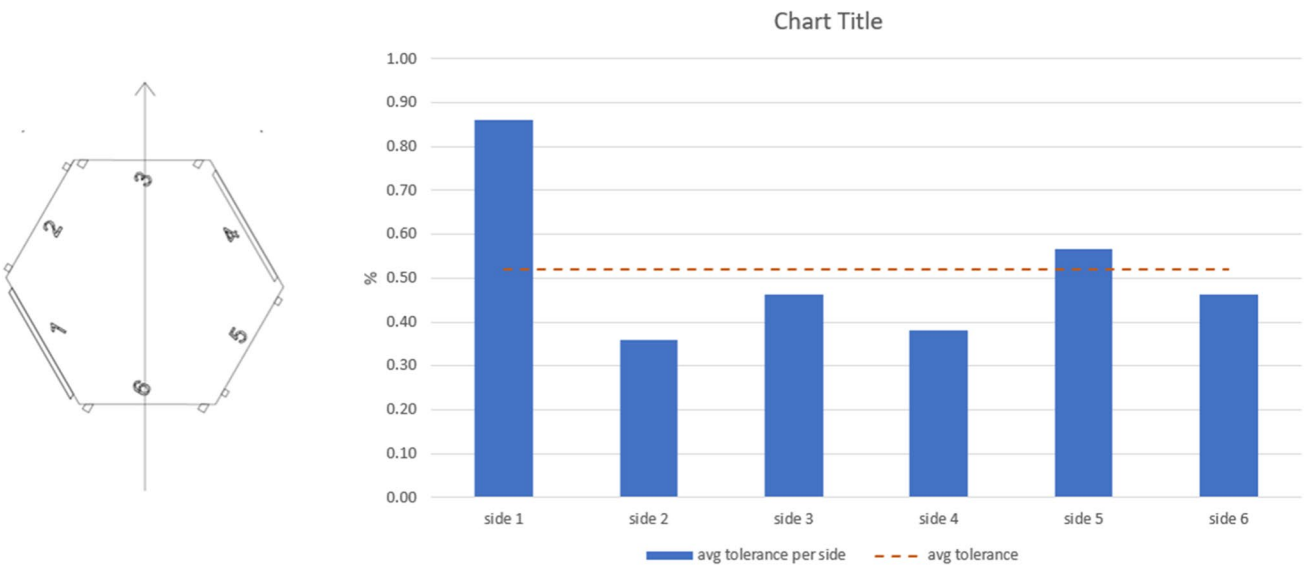

Fig. 8 Average deviation of dimensions per side of panel. The arrow on the left side shows the printing direction

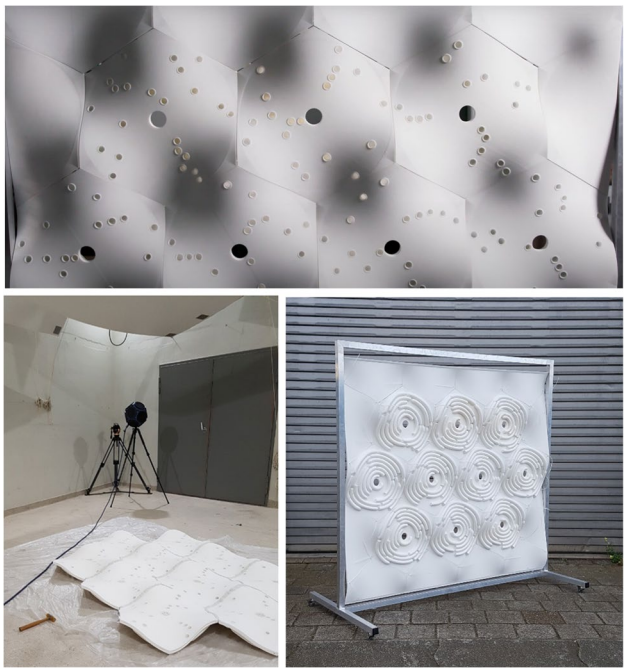

Fig. 9 Case Study 2 [TOP] assembled panel front view, [BOTTOM LEFT] measurements of case 3 in the reverberation room and [BOTTOM RIGHT] assembled panel back view

a diffuse field can be derived. The results for case 2 are overall very similar to the results for case 1: the panels (Fig. 10, green curve – open tubes relative to the empty room) show broadband absorption at the targeted frequency range (240–315 Hz) that is consistent with theory. Even though the number of resonators is the same and they are tuned for the same frequencies, the peaks are slightly lower for this case. This result was expected due to the 20% increase in the 3D printed surface. The same effect can also be observed in the theoretically computed results.

The results for the panels with tubes closed by clay (relative to the empty room) indicate sound absorption coefficient values generally between 0.2 to 0.4 (Fig. 10, red curve – closed tubes relative to an empty room). As previously, the panels' resonance is likely responsible for this result.

Discussion

The computational workflow used in this work, which consisted of two main steps (the optimisation tool and the TADO), was tested in two case studies: for flat and 3D surfaces. For both cases, the computational workflow was the same and the acoustic performance was validated via measurements; however, each case examined a different version of the design tool, with TADO1 used for flat surfaces and TADO2 for 3D surfaces. Both processes ran in Rhino/Grasshopper software. Performing the optimisation and design steps in the same environment allows unlimited experimental iterations of the design in terms of both form and performance refinement. The automated design workflow used in this study simplifies the geometry generation process, which would be labour-intensive if performed manually. Furthermore, the computational tool used to automate the process of form customisation, via free-form shapes, and optimising acoustic performance is beneficial for increasing the quality of a space, thus maximising the benefits and harnessing the potential of the AM technique.

In case 1, the designed sound absorber is flat and very compact. The simplicity of its geometry makes it possible to pack the tubes compactly. This solution is suitable for applications where high performance and space limitations are the main design drivers for the room acoustics, e.g. aircraft cabins and office buildings. In case 2, the 3D surface demands more volume which thus increases production costs. Additionally, the tubes are arranged in a less dense layout. However, the 3D shape of the panel may be beneficial for sound diffusion. This solution is more suitable for applications where performance is paramount in combination with visual aspects, such as in meeting rooms and entrance halls. Even though the 3D volume in this case might be less efficient in packaging the tubes, it offers more possibilities in terms of architectural applications.

The production technique in this study was chosen because of sustainability criteria. The powder-based technique is also more suitable for producing hollow tube structures without the need for support structures, and it involves reduced post-processing times. Because of the size of the panels, some shrinkage was observed in their dimensions. This deviation in dimensions from the original design specification may have caused some inaccuracies in the measurements. In addition, negatively affects the assembly of the panels. In future studies, this tolerance must be integrated into the design.

For the measurements in the reverberation room, a custom analysis technique was developed allowing for high-resolution results. As a result, it was possible to analyse the sound absorption coefficient in a diffuse field in a high level of detail. The results show that the performance of open tube structures can be predicted based on the theory of visco-thermal wave propagation in a diffuse field. The remaining small discrepancies between the analytical and experimental results may relate to the size of the sample, the edge effect, the material properties of the examined resonators, measuring inaccuracies, imperfections in the prototype and approximation of the effective length of the air path. Future research should focus on eliminating these aspects by working with larger samples, better sealing of the sample edges, etc., to improve the reliability of the results. It would be recommended to test samples of larger surfaces and comply with the international standards concerning that.

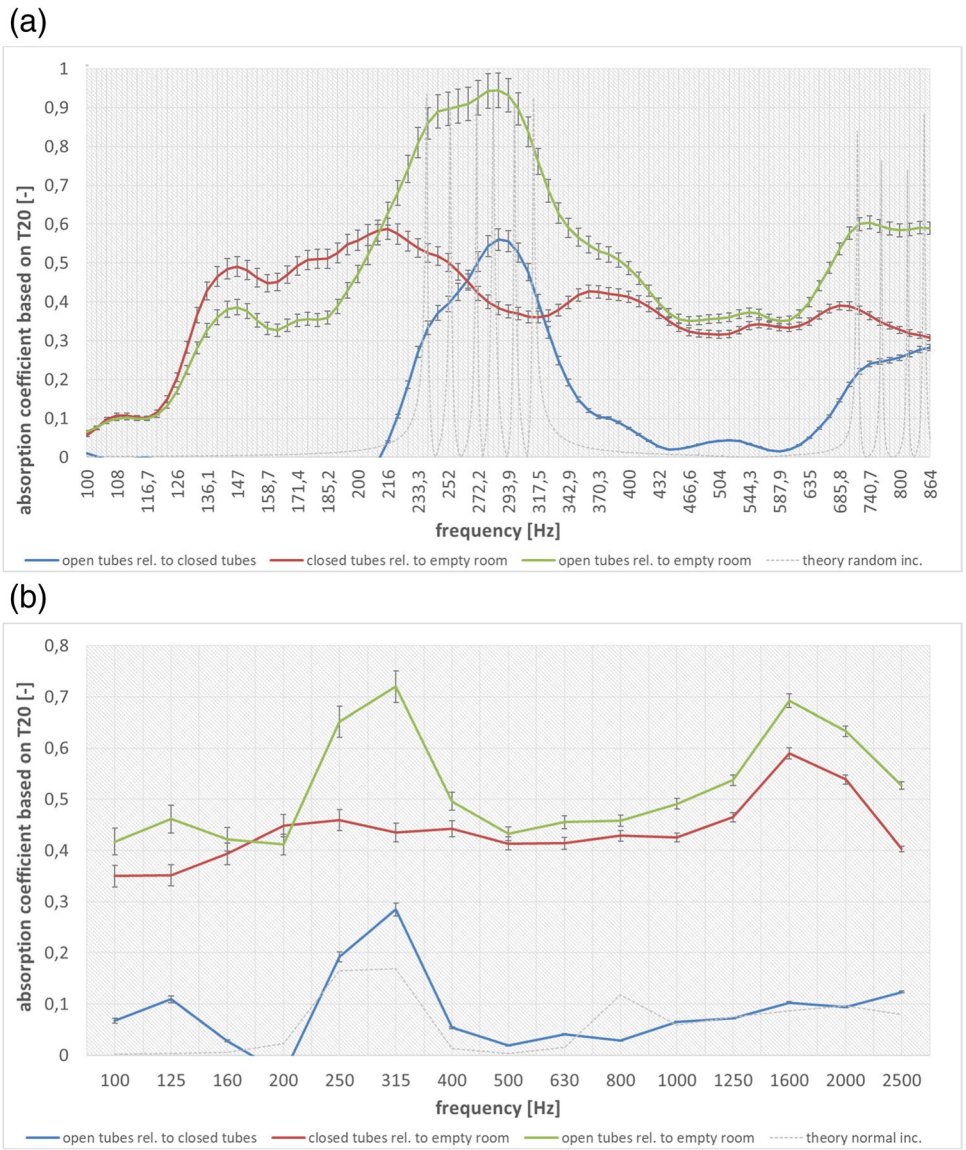

Fig. 10 Case 2: measured vs calculated performance of the sound absorption coefficient analysed in (**a**) 1/27th and (**b**) 1/3rd octave bands. The theoretical curves in the 1/27th octave bands graph are based on a continuous theoretical function and in the 1/3rd octave band graphs are filtered for 1/3rd octave bands

Conclusions

This paper demonstrated the possibility of producing compact resonant absorber panels for low frequencies by taking advantage of AM. Due to the bending of the tubes, the thickness of the samples became significantly smaller than the corresponding targeted wavelength (approximately 1/30 for case 1 and 1/10 for case 2). For future research, an area of interest would be to explore further applications of this design and technology combination: the ability to address broadband absorption at low frequencies, in compact sizes and custom shapes, opens new possibilities in terms of multifunctional components with integrated functionalities such as lighting, air diffusion and high-frequency absorption.

Acknowledgements The ADAM project was part of the Open Technology research program with project number 13704, which was financed by the Netherlands Organization for Scientific Research (NWO). Other project partners include Materialise, Peutz, Merford and ARUP. Special thanks to Lau Nijs, Evert de Ruiter and Diemer de Vries.

Declarations

Conflict of interest The authors declare that they have no conflict of interest.

References

1. 3DHubs (2020) Retrieved from https://www.3dhubs.com/knowledge-base/dimensional-accuracy-3d-printed-parts/#sls. Accessed 11/02/2023
2. Carvalho AP, Sousa MR (2016) Effect of sample area in reverberant chamber measurements of sound absorption coefficients. In 22nd International Congress on Acoustics
3. Cox T, D'Antonio P (2009) Acoustic absorbers and diffusers: theory, design and application (2nd ed.). Taylor & Francis, London; New York
4. Eerden F (2000) Noise reduction with coupled prismatic tubes. University of Twente, Enschede
5. Fotsing ER, Dubourg A, Ross A, Mardjono J (2019) Acoustic properties of periodic micro-structures obtained by additive manufacturing. Appl Acoust 148:322–331
6. Fuchs HV (2013) Applied acoustics: concepts, absorbers, and silencers for acoustical comfort and noise control: alternative solutions-Innovative tools-Practical examples. Springer Science & Business Media
7. Godbold OB, Soar RC, Buswell RA (2007) Implications of solid freeform fabrication on acoustic absorbers. Rapid Prototyp J 13(5):298–303
8. Gomes PC, Piñeiro OG, Alves AC, Carneiro OS (2022) On the reuse of SLS polyamide 12 powder. Materials 15(16):5486
9. Gramazio K (2020) Gramazio Kohler research, ETH Zurich. Retrieved from https://gramaziokohler.arch.ethz.ch/web/e/forschung/342.html. Accessed 11/02/2023
10. ISO 354:2003 Acoustics — Measurement of sound absorption in a reverberation room
11. Lee HM, Wang Z, Lim KM, Lee HP (2020) Investigation of the effects of sample size on sound absorption performance of noise barrier. Appl Acoust 157:106989
12. Lee H, Tsuchiya Y, Sakuma T (2018) Acoustic scattering characteristics of Penrose-tiling-type diffusers. Appl Acoust 130:168–176
13. Reinhardt D (2018) The sound of space in 3 robotic prototypes: introducing 6-axis robotic fabrication to shape macroand micro-geometries for acoustic performance. A| Z ITU J Fac Archit 15(1):79–92
14. Setaki F, Tenpierik M, Turrin M, Timmeren A (2016) New sound absorption materials: using additive manufacturing for compact size, broadband sound absorption at low frequencies. Inter-noise and noise-con congress and conference proceedings. Inst Noise Control Eng 253(2):6190–6195
15. Tian F, Setaki F, Turrin M, Tenpierik M, Timmeren A (2019) ADAM final project report: automatic design, optimization and geometric modeling of two-dimensional acoustic absorption panels with arbitrary shapes based on knowledge-based engineering
16. Vidakis N, Petousis M, Tzounis L, Maniadi A, Velidakis E, Mountakis N, Kechagias JD (2021) Sustainable additive manufacturing: Mechanical response of polyamide 12 over multiple recycling processes. Materials 14(2):466
17. Vomhof M, Vasey L, Brauer S, Eggenschwiler K, Strauss J, Gramazio F, Kohler M (2014) Robotic fabrication of acoustic brick walls. ACADIA 14: design agency [Proceedings of the 34th Annual Conference of the Association for Computer Aided Design in Architecture (ACADIA) Los Angeles 23–25, pp. 555–564. Retrieved from https://gramaziokohler.arch.ethz.ch/web/e/forschung/229.html
18. Zwikker C, Kosten C (1949) Sound absorbing materials. Elsevier, New York